The Seventh Transmembrane Domains of the δ and κ Opioid Receptors Have Different Accessibility Patterns and Interhelical Interactions

Wei Xu,[‡] Mercedes Campillo,[§] Leonardo Pardo,[§] J. Kim de Riel,[||] and Lee-Yuan Liu-Chen*[,‡]

Department of Pharmacology and Center for Substance Abuse Research and Fels Institute for Molecular Biology and Cancer Research, Temple University School of Medicine, Philadelphia, PA 19140, and Laboratori de Medicina Computacional, Unitat de Bioestadística and Institut de Neurociències, Universitat Autònoma de Barcelona, 08193 Bellaterra, Barcelona, Spain

Received May 20, 2005; Revised Manuscript Received October 12, 2005

ABSTRACT: We applied the substituted cysteine accessibility method (SCAM) to map the residues of the transmembrane helices (TMs) 7 of δ and κ opioid receptors (δOR and κOR) that are on the water-accessible surface of the binding-site crevices. A total of 25 consecutive residues (except C7.38) in the TMs 7 were mutated to Cys, one at a time, and each mutant was expressed in HEK 293 cells. Most mutants displayed similar binding affinity for [^{3}H]diprenorphine, an antagonist, as the wild types. Pretreatment with (2-aminoethyl)methanethiosulfonate (MTSEA) inhibited [^{3}H]diprenorphine binding to eight δOR and eight κOR mutants. All mutants except δOR L7.52(317)C were protected by naloxone from the MTSEA effect, indicating that the side chains of V7.31(296), A7.34(299), I7.39(304), L7.41-(306), G7.42(307), P7.50(315), and Y7.53(318) of δOR and S7.34(311), F7.37(314), I7.39(316), A7.40-(317), L7.41(318), G7.42(319), Y7.43(320), and N7.49(326) of κOR are on the water-accessible surface of the binding pockets. Combining the SCAM data with rhodopsin-based molecular models of the receptors led to the following conclusions. (i) The residues of the extracellular portion of TM7 predicted to face TM1 are sensitive to MTSEA in κOR but are not in δOR. Thus, TM1 may be closer to TM7 in δOR than in κOR. (ii) MTSEA-sensitive mutants start at position 7.31(296) in δOR and at 7.34(311) in κOR, suggesting that TM7 in δOR may have an additional helical turn (from 7.30 to 7.33). (iii) There is a conserved hydrogen-bond network linking D2.50 of the NLxxxD motif in TM2 with W6.48 of the CWxP motif in TM6. (iv) The NPxxY motif in TM7 interacts with TM2, TM6, and helix 8 to maintain receptors in inactive states. To the best of our knowledge, this represents the first such comparison of the structures of two highly homologous GPCRs.

More than 1000 G protein-coupled receptors (GPCRs)[1] are present in the human genome. GPCRs play important roles in physiological functions, including smell, taste, light perception, neurotransmission, functions of endocrine and exocrine glands, and immune functions. In addition, GPCRs are targets of numerous clinically used drugs. It is, therefore, of great interests to understand their structures at the molecular level. On the basis of structural characteristics, GPCRs are classified into multiple families, and the rhodopsin family is by far the largest in number. To date, rhodopsin is the only GPCR of which high-resolution crystal structures have been elucidated (*1*−*3*). Rhodopsin has an extracellular N-terminal domain, seven transmembrane helices (TMs) connected by alternating intra- and extracellular hydrophilic loops and an intracellular C-terminal domain. A short helix, helix 8 (H8), parallel to the plane of plasma membranes is present in the proximal region of the C-terminal domain. GPCRs of the rhodopsin family are thought to have similar 7-TM bundles (*4*, *5*).

Opioid receptors mediate effects of opiate and opioid compounds, which are important therapeutic agents for pain management. Multiple opioid receptors (at least μ, δ, and κ) have been defined pharmacologically. After the cloning of the mouse δ opioid receptor, μ and κ receptors were cloned (refs *6* and *7* and references therein). These receptors belong in the rhodopsin family (family A) of GPCRs. These opioid receptors are coupled through pertussis-toxin-sensitive G proteins to affect a variety of effectors (for a review, see ref *8*). Several groups have constructed molecular models of opioid receptors (for example, see refs *9*−*12*).

Results from experimental probes have indicated that binding pockets of GPCRs involve the seven TMs and are accessible from the extracellular medium. Some water-accessible residues within the binding pocket directly interact with ligands. Javitch and his colleagues have used charged, hydrophilic methanethiosulfonate (MTS) reagents, which react specifically with reduced sulfhydryl groups, to identify

* To whom correspondence should be addressed: Department of Pharmacology, Temple University School of Medicine, 3420 N. Broad St., Philadelphia, PA 19140. Telephone: (215) 707-4188. Fax: (215) 707-7068. E-mail: lliuche@temple.edu.

[‡] Department of Pharmacology and Center for Substance Abuse Research, Temple University School of Medicine.

[§] Universitat Autònoma de Barcelona.

[||] Fels Institute for Molecular Biology and Cancer Research, Temple University School of Medicine.

[1] Abbreviations: TM, transmembrane helix; H8, helix 8; δOR and κOR, δ and κ opioid receptors; SCAM, substituted cysteine accessibility method; MTS, methanethiosulfonate; MTSEA, (2-aminoethyl)methanethiosulfonate; GPCR, G protein-coupled receptor; TEL buffer, 50 mM Tris-HCl buffer containing 1 mM EGTA and 10 μM leupeptin (pH 7.4); Kreb's solution, 130 mM NaCl, 4.8 mM KCl, 1.2 mM KH_2PO_4, 1.3 mM $CaCl_2$, 1.2 mM $MgSO_4$, 10 mM glucose, and 25 mM HEPES at pH 7.4; e3 loop, third extracellular loop; e2 loop, second extracellular loop.

10.1021/bi050938a CCC: $30.25
Published on Web 11/16/2005

Cys residues accessible in the binding pocket of the D_2 dopamine receptor and applied the substituted cysteine accessibility method (SCAM) to map residues within the TMs of this receptor exposed in the binding-site crevice (for reviews, see refs *5* and *13*). We have also employed SCAM to identify and compare residues accessible in the binding-site crevice in the TMs 6 of the μ, δ, and κ opioid receptors (*14*). MTS reagents react10^9 times faster with ionized thiolates (S^-) than with un-ionized thiols (SH) (*15*), and ionization of cysteine occurs to a significant extent only in the aqueous medium (*16*). Thus, the reaction rate of these MTS reagents is expected to be much faster with cysteine residues at the water-accessible surface than with those that are not. SCAM analysis involves substitution of each residue with cysteine within a TM one at a time, and the effects of the reaction with MTS reagents on ligand binding were determined. Those that result in binding inhibition are inferred to be on the water-accessible binding-site crevice.

Studies have been performed to characterize the interaction of ligands with opioid receptors. The region of the TMs 6 and 7 and the third extracellular (e3) loop was demonstrated to play important roles in ligand-binding selectivity of μ, δ, and κ opioid receptors by site-directed mutagenesis and chimeric receptor studies (for example, see refs *17*−*20*).

TMs 7 of the rhodopsin family of GPCRs have been documented to play important roles in maintaining receptors in inactive states. Disruption of an ionic interaction between a positively charged residue in TM7 and a negatively charged residue in TM3 in rhodopsin (*21*), α_{1b}-adrenergic (*22*), and δ opioid (*23*) receptors leads to constitutive activation. Hydrogen-bonding interactions between TM2 and TM7 have been suggested to be important for the activity of gonadotropin-releasing hormone, 5-hydroxytryptamine$_{2A}$ (5-HT_{2A}), and μ opioid receptors (*24*−*26*). In addition, there is an interaction between Y7.53 in TM7 and an aromatic residue F/Y7.60 in H8 of the $NPXXYX_{5-6}F/Y7.60$ motif in the inactive states of rhodopsin (*27*) and the $5HT_{2C}$ receptor (*28*).

We have shown that μ, δ, and κ opioid receptors are differentially sensitive to MTSEA, $CH_3SO_2SCH_2CH_2NH_3^+$, in the order of $\kappa > \mu > \delta$, and the conserved Cys7.38 largely confers the MTSEA sensitivity in each receptor (*29*). While C7.38 in the μ and κ receptors is readily accessible from the binding-site crevice, this conserved residue in the δ receptor appears to be much less accessible (*29*). In the present study, we applied the SCAM to further explore the differential exposure of C7.38 to the binding-site crevice and identify and compare the amino acid residues within the TM 7 of the δOR and κOR that are accessible from the extracellular medium. In addition, the experimental results are interpreted in the context of rhodopsin-based computational models of the δOR and κOR. These comparative results serve to identify unique features in the δOR and κOR as well as common structural patterns in GPCRs. A comparison of amino acid sequences of TMs 7 of the δOR and κOR and rhodopsin is shown in Figure 1.

```
brho   7.33(286) IFMTIPAFFAKTSAVYNPVIYIMM 7.56(309)
hdor 7.31(296) VVAALHLCIALGYANSSLNPVLYAFL 7.56(321)
hkor 7.31(308) ALSSYYFCIALGYTNSSLNPILYAFL 7.56(333)
```

FIGURE 1: Amino acid sequence alignment of TMs 7 of the human δOR and κOR and bovine rhodopsin(brho).

EXPERIMENTAL PROCEDURES

Materials. [^{3}H]Diprenophine (58 Ci/mmole) was purchased from Perkin−Elmer Co. (Boston, MA). Naloxone was a gift from the former DuPont/Merck Co. (Wilmington, DE). MTSEA was purchased from Toronto Research Chemicals (North York, Ontario, Canada). Enzymes and chemicals used in molecular biology and mutagenesis experiments were purchased from Life Technologies Co. (Gaithersburg, MD), Promega (Madison, WI), Bohringer-Mannheim Co. (Indianapolis, IN), and Qiagen Co. (Valencia, CA).

Numbering Schemes for Amino Acid Residues in Opioid Receptors. Two numbering schemes were used. Amino acid residues in the δOR and κOR are identified by their sequence numbers. In addition, the generic numbering scheme of amino acid residues in GPCRs according to Ballesteros and Weinstein (*30*) is used. According to this nomenclature, the most conserved residue in the TM7 of human δ and human κ ORs is Pro7.50 (δ, Pro315; κ, Pro327). The boundary for the TMs 7 of δOR and κOR is 7.31−7.56 (δ, V296−L321; κ, A308−L333) based on the models of Strahs and Weinstein (*9*) with modifications. The generic numbering allows for an easy comparison among the opioid receptors and a cross-reference to other GPCRs in the literature.

Oligodeoxynucleotide-Directed Mutagenesis. Site-directed mutagenesis was performed on the C7.38(315)S mutants of the human κ receptors and the wild-type human δ OR with the overlap PCR method described by Higuchi et al. (*31*). FLAG-tagged human wild-type and mutant δ receptors were subcloned into *Eco*R I and *Bam*H I sites of the vector pIRESneo (originally described as pCIN4). FLAG-tagged human wild-type and mutant κ receptors were subcloned into *Hin*d III and *Xho* I sites of the vector pcDNA3 (*29*). The DNA sequence was determined to confirm the presence of desired mutations and the absence of unwanted mutations.

Transfection of HEK293 Cells. HEK 293 cells were grown in 100-mm culture dishes in Minimum Essential Medium supplemented with 10% fetal calf serum, 100 units/mL penicillin, and 100 μg/mL streptomycin in a humidified atmosphere consisting of 5% CO_2 and 95% air at 37 °C. Cells were transfected with the wild type or a mutant of κOR DNA (5 μg/dishes plus 15 μg of vector) using the calcium phosphate method (*32*). A total of 60−72 h after transfection, cells were harvested for experiments by detaching with Versene solution. Transfection of HEK cells with the DNA clones of the wild type or a mutant of the human δOR in pIRESneo was performed with Lipofectamine according to the instructions of the manufacturer. Cells were grown under the selection pressure of geneticin (0.8 mg/mL), and nearly all surviving colonies stably expressed the receptor.

Determination of K_d and B_{max} Values of [^{3}H]Diprenorphine Binding. Membranes were prepared from transfected HEK cells as described previously (*33*). Saturation binding of [^{3}H]diprenorphine to the wild-type and mutant δ and κ receptors was performed with at least six concentrations of [^{3}H]diprenorphine (ranging from 25 pM to 2 nM), and K_d and B_{max} values were determined. Binding was carried out in 50 mM Tris-HCl buffer containing 1 mM EGTA and 10 μM leupeptin (pH 7.4) (TEL buffer) at room temperature for 1 h in duplicate in a volume of 1 mL with ∼10−20 μg of membrane protein. Naloxone (10 μM) was used to define nonspecific binding. Binding data were analyzed with the EBDA programs (*34*).

Reaction with MTSEA. The experiments were performed according to our published procedure (*14*). Transfected cells were detached by use of the Versene solution, pelleted at 1000*g* for 1 min at room temperature, and washed with Kreb's solution (130 mM NaCl, 4.8 mM KCl, 1.2 mM KH_2PO_4, 1.3 mM $CaCl_2$, 1.2 mM $MgSO_4$, 10 mM glucose, and 25 mM HEPES at pH 7.4) and centrifuged again. The pellets were resuspended in Kreb's solution, and aliquots of cell suspension were incubated with freshly prepared MTSEA at the stated concentration in a final volume of 0.5 mL at room temperature for 5 min. The reaction was stopped by adding 0.5 mL of 0.8% bovine serum albumin (BSA) solution. The cell suspensions were pelleted and washed once with Kreb's solution. After centrifugation, the pellet were resuspended in 1 mL/dish Kreb's solution and 50 μL aliquots were used for [^{3}H]diprenorphine binding to intact cells at room temperature for 1 h as described previously (*35*). Naloxone (10 μM) was used to define nonspecific binding. The percent inhibition was calculated as [1 − (specific binding after the MTS reagent/specific binding without the reagent)] × 100%. Data were analyzed by one-way ANOVA followed by post hoc Sheffe *F* test using $p < 0.05$ as the level of significance.

Determination of Second-Order Rate Constants. The second-order rate constants of the interaction between the δOR or κOR mutants and MTSEA was determined to gain quantitative information on MTSEA sensitivity, according to our published method (*36*). Cells expressing a mutant receptor were incubated with indicated concentrations of MTSEA for 5 min. The results were fit to the equations:

$$Y = (\text{extent of inhibition})e^{-kct} + \text{plateau}$$

$$\text{extent of inhibition} + \text{plateau} = 1.0$$

where Y is the fraction of the initial binding, k is the second-order rate constant (M^{-1} s^{-1}), c is the concentration of MTSEA (M), and t is the incubation time (300 s).

Protection by Naloxone Against the MTSEA Reaction. Dissociated cells were incubated with indicated concentrations of naloxone for 20 min for binding to the δ and κ receptors to reach equilibrium. Cells were then treated with a concentration of MTSEA that was just sufficient to achieve maximal inhibition of binding to each receptor. Cells were washed 3 times by centrifugation and then resuspended in Kreb's solution and assayed for [^{3}H]diprenorphine binding.

Determination of the Protein Content. Protein contents of membranes were determined by the bicinchoninic acid method of Smith et al. (*37*) with BSA as the standard.

Construction of Molecular Models of the δOR and κOR. Models of the δOR and κOR were constructed by homology modeling using the crystal structure of bovine rhodopsin (PDB code 1GZM) (*2*) as a template. Included in the models are the TMs 1−7, the intracellular loops 1−3, the extracellular loops 1−3, the second extracellular (e2) loop forming the disulfide-bonded cysteine to TM5, and the H8 that expands parallel to the membrane. The residues considered to be most conserved in the class A family of GPCRs were aligned and assigned as #0.50, in which # represents the TM according to the nomenclature of Ballesteros and Weinstein (*30*). These include D2.50 (rhodopsin-83, δ-95, κ-105), R3.50 (rhodopsin-135, δ-146, κ-156), W4.50 (rhodopsin-161,δ-173, κ-183), P5.50 (rhodopsin-215, δ-225, κ-238), P6.50 (rhodopsin-267, δ-276, κ-289), and P7.50 (rhodopsin-303, δ-315, κ-327). Opioid receptors contain the T2.56-X-P2.58 motif in TM2. This motif orients the extracellular moiety of TM2 toward TM3 (*38*). Therefore, TM2 and TM3 were modeled as suggested for the chemokine CCR5 receptor (*39*). Water molecules 2, 7, and 9 observed in the D2.50/N7.49/Y7.53 environment of rhodopsin (*2*) are also included in the model. SCWRL-3.0 was employed to add the side chains of the nonconserved residues based on a backbone-dependent rotamer library (*40*). These molecular models were placed in a rectangular box (∼80 × 93 × 75 Å in size) containing a lipid bilayer (∼95 molecules of palmitoyloleoylphosphatidylcholine and ∼13 000 molecules of water) resulting in a final density of ∼1.0 g cm^{-3}.

The receptor−lipid bilayer systems were subjected to 500 iterations of energy minimization and then heated to 300 K in 15 ps. This was followed by an equilibration period (15−250 ps) and a production run (250−500 ps) at constant pressure with anisotropic scaling, using the particle mesh Ewald method to evaluate the electrostatic interaction. During the processes of minimization, heating, and equilibration, a positional restraint of 10 kcal mol^{-1} $Å^{-2}$ was applied to the C_α atoms of the receptor structure. This simulation protocol seems adequate to adapt the rhodopsin template to the structural requirements of the opioid receptor side chains, with the aim of understanding the local helix−helix interactions. Structures were collected for analysis every 10 ps during the production run (25 structures/simulation). Representative structures for each trajectory were selected by automatically clustering the collected geometries into conformationally related subfamilies with NMRCLUST (*41*). The molecular dynamics (MD) simulations were run with the Sander module of AMBER 8 (*42*), the ff99 force field (*43*), a 2 fs integration time step, and a constant temperature of 300 K.

RESULTS

Effect of Cysteine Substitutions on the Affinity of the δOR and κOR for [^{3}H]Diprenorphine. Each residue in the TMs 7 was mutated to cysteine, one at a time, and mutant receptors were expressed in HEK293 cells. Saturation binding of [^{3}H]diprenorphine to each mutant was performed on intact cells with naloxone to define nonspecific binding, and K_d and B_{max} values were determined (Tables 1 and 2). It should be noted that both [^{3}H]diprenorphine and naloxone can penetrate cell membranes; therefore, the binding assay detected both cell surface and intracellular receptors. S7.46-(311)C mutation in the δOR and P7.50(327)C mutation in the κOR abolished [^{3}H]diprenorphine binding, although immunoblotting using anti-FLAG antibody showed that both mutants were expressed (data not shown). K_d values of [^{3}H]-diprenorphine binding to all other κOR and δOR mutants ranged from 0.3- to 2.1-fold of that of the δOR wild type and from 0.5- to 4.3-fold of that of the κOR C7.38S mutant, respectively (Tables 1 and 2), indicating that these mutants have similar affinities for [^{3}H]diprenorphine as the wild type. We also generated the S7.46(311)A mutant of the δOR and found that this mutant bound [^{3}H]diprenorphine with a similar affinity as the wild type. Thus, most mutations did not affect the binding pockets substantially. The mutants were expressed to different levels (Tables 1 and 2). These results suggest that most substituted cysteine side chains may have

Table 1: K_d and B_{max} of [^{3}H]Diprenorphine Binding to the Cysteine-Substituted δOR Mutants Expressed in HEK 296 Cells[a]

mutant	K_d (nM)	$K_m/K_{C7.38S}$	B_{max} (pmol/mg of protein)
V7.31(296)C	0.38 ± 0.03	1.1	10.2 ± 0.18
V7.32(297)C	0.26 ± 0.03	0.7	4.5 ± 0.32
A7.33(298)C	0.21 ± 0.06	0.6	0.39 ± 0.05
A7.34(299)C	0.26 ± 0.05	0.7	0.11 ± 0.02
L7.35(300)C	0.49 ± 0.08	1.4	1.1 ± 0.04
H7.36(301)C	0.25 ± 0.01	0.7	0.05 ± 0.01
L7.37(302)C	0.28 ± 0.02	0.8	2.4 ± 0.31
C7.38(303)/WT	**0.35 ± 0.07**	1.0	**3.5 ± 0.20**
I7.39(304)C	0.16 ± 0.01	0.4	1.06 ± 0.04
A7.40(305)C	0.21 ± 0.04	0.6	0.33 ± 0.03
L7.41(306)C	0.21 ± 0.02	0.6	0.52 ± 0.14
G7.42(307)C	0.61 ± 0.11	1.7	0.62 ± 0.05
Y7.43(308)C	0.69 ± 0.19	1.9	0.06 ± 0.01
A7.44(309)C	0.28 ± 0.01	0.8	2.0 ± 0.08
N7.45(310)C	0.68 ± 0.15	1.9	0.20 ± 0.02
S7.46(311)C	no binding was detected		
S7.47(312)C	0.28 ± 0.01	0.8	3.1 ± 0.06
L7.48(313)C	0.23 ± 0.03	0.6	0.43 ± 0.03
N7.49(314)C	0.32 ± 0.03	0.9	0.42 ± 0.01
P7.50(315)C	0.74 ± 0.12	2.1	0.42 ± 0.21
V7.51(316)C	0.23 ± 0.03	0.6	3.9 ± 0.37
L7.52(317)C	0.23 ± 0.03	0.6	0.35 ± 0.03
Y7.53(318)C	0.12 ± 0.01	0.3	0.07 ± 0.01
A7.54(319)C	0.31 ± 0.01	0.8	4.2 ± 0.07
F7.55(320)C	0.20 ± 0.02	0.5	1.5 ± 0.09
L7.56(321)C	0.35 ± 0.02	1.0	0.57 ± 0.02

[a] Saturation binding of [^{3}H]diprenorphine to the cysteine-substituted δOR mutants was performed, and K_d and B_{max} values were calculated as described in the Experimental Procedures.

Table 2: K_d and B_{max} of [^{3}H]Diprenorphine Binding to the Cysteine-Substituted κOR Mutants Expressed in HEK 296 Cells[a]

mutant	K_d (nM)	$K_m/K_{C7.38S}$	B_{max} (pmol/mg of protein)
A7.31(308)C	1.43 ± 0.07	4	1.2
L7.32(309)C	0.48 ± 0.03	1.4	2.1
S7.33(310)C	0.32 ± 0.12	0.9	1.5
S7.34(311)C	0.28 ± 0.15	0.8	1.9
Y7.35(312)C	0.17 ± 0.04	0.5	0.22
Y7.36(313)C	0.88 ± 0.01	2.5	1.2
F7.37(314)C	0.18 ± 0.02	0.5	0.8
C7.38(315)S	**0.35 ± 0.03**		**1.5**
I7.39(316)C	0.68 ± 0.14	1.9	2.1
A7.40(317)C	0.23 ± 0.05	0.7	0.52
L7.41(318)C	0.33 ± 0.02	0.9	0.15
G7.42(319)C	0.66 ± 0.01	1.9	0.8
Y7.43(320)C	0.37 ± 0.09	1.1	0.03
T7.44(321)C	0.48 ± 0.37	1.4	1.6
N7.45(322)C	0.68 ± 0.15	1.9	2.4
S7.46(323)C	1.10 ± 0.12	3.1	1.7
S7.47(324)C	0.29 ± 0.08	0.8	1.6
L7.48(325)C	1.35 ± 0.06	3.9	1.8
N7.49(326)C	0.70 ± 0.04	2	0.93
P7.50(327)C	no binding was detected		
I7.51(328)C	0.48 ± 0.08	1.4	2.0
L7.52(329)C	0.39 ± 0.03	1.1	0.62
Y7.53(330)C	1.52 ± 0.05	4.3	0.74
A7.54(331)C	0.53 ± 0.06	1.5	1.35
F7.55(332)C	0.28 ± 0.05	0.8	1.14
L7.56(333)C	0.31 ± 0.07	0.9	0.59

[a] Saturation binding of [^{3}H]diprenorphine to the cysteine-substituted κOR mutants was performed, and K_d and B_{max} values were calculated as described in the Experimental Procedures.

similar orientations as the residues being replaced at the same positions, which is the basis for SCAM analysis.

Cell-Surface Expression of the Wild Type and Mutant δOR and κOR. Intact cells were used in the study because it is necessary to limit the MTSEA reaction to −SH groups accessible from the extracellular medium. Whether receptor constructs were expressed on the cell surface is an important issue. We determined the percent of each wild-type and mutant receptor expressed on the cell surface by ligand binding. Total and cell-surface receptor binding were performed with 0.2−0.4 nM [^{3}H]diprenorphine. For total receptors, nonspecific binding was defined as the binding in the presence of 10 μM naloxone. For the cell-surface receptor, nonspecific binding was defined by 10 μM dynorphin A(1−17) and 10 μM DPDPE for the κ and δ receptors, respectively (*35*, *44*). Naloxone, being highly hydrophobic, is able to penetrate cell membranes, whereas both dynorphin A(1−17) and DPDPE are hydrophilic and thus unable to go through plasma membranes. We found that for all mutant and wild-type receptors that exhibited binding activities, 70−80% of the receptors were expressed on cell surface. It should be noted that each of the wild-type and mutant FLAG-κOR and FLAG-δOR constructs contains an amino-terminal cleavable signal peptide sequence, which enhances translocation of the receptor into the endoplasmic reticulum membrane and thus facilitates expression of the functional receptor in plasma membranes (*45*).

Effect of MTSEA Pretreatment on [^{3}H]Diprenorphine Binding to the Cysteine Mutants of the δOR and κOR. A total of 8 of the 25 cysteine-substituted mutants of the δOR were sensitive to MTSEA: V7.31(296), A7.34(299), I7.39-(304), L7.41(306), G7.42(307), P7.50(315), L7.52(317), and Y7.53(318) (Figure 2). In addition, pretreatment with MTSEA significantly inhibited [^{3}H]diprenorphine binding to 8 of the 25 cysteine-substituted mutants of the κOR: S7.34-(311), F7.37(314), I7.39(316), A7.40(317), L7.41(318), G7.42(319), Y7.43(320), and N7.49(326) (Figure 2).

Protective Effect of Naloxone against the Inhibitory Action of MTSEA. All of the MTSEA-sensitive mutants (from Figure 2), except the δOR L7.52C mutant, were protected by naloxone from MTSEA alkylation (Figure 3), indicating that V7.31(296), A7.34(299), I7.39(304), L7.41(306), G7.42-(307), P7.50(315), and Y7.53(318) of the δOR and S7.34-(311), F7.37(314), I7.39(316), A7.40(317), L7.41(318), G7.42(319), Y7.43(320), and N7.49(326) of the κOR are on the water-accessible surface of the binding-site crevice. In addition, we showed previously that C7.38(318) of the κOR was exposed in the binding pocket but C7.38(303) of the δOR was not (*29*).

Determination of Second-Order Rate Constants of MTSEA Reactions with Sensitive Mutants. To quantitatively express the inhibitory potency of MTSEA on [^{3}H]diprenorphine binding to MTSEA-sensitive mutants of the δOR and κOR, we determined the second-order rate constants (Table 3). The κOR mutants, except the 7.42C mutant, have much higher reaction rates than the δOR mutants. For the κOR mutants, the rate constants were in the order of 7.39C ≫> 7.40C > 7.34C, 7.37C, 7.41C > 7.43C >7.42C >7.49C. For the δOR mutants, the rank order of the rate constant was 7.39C > 7.42C, 7.50C > 7.31C, 7.34C, 7.41C > 7.53C.

Molecular Models of the δOR and κORs. Figure 4A shows the result of superimposing the initial structure of the molecular dynamic simulation of the δOR (in tube ribbon) and the rhodopsin template. The κOR is similar to the δOR

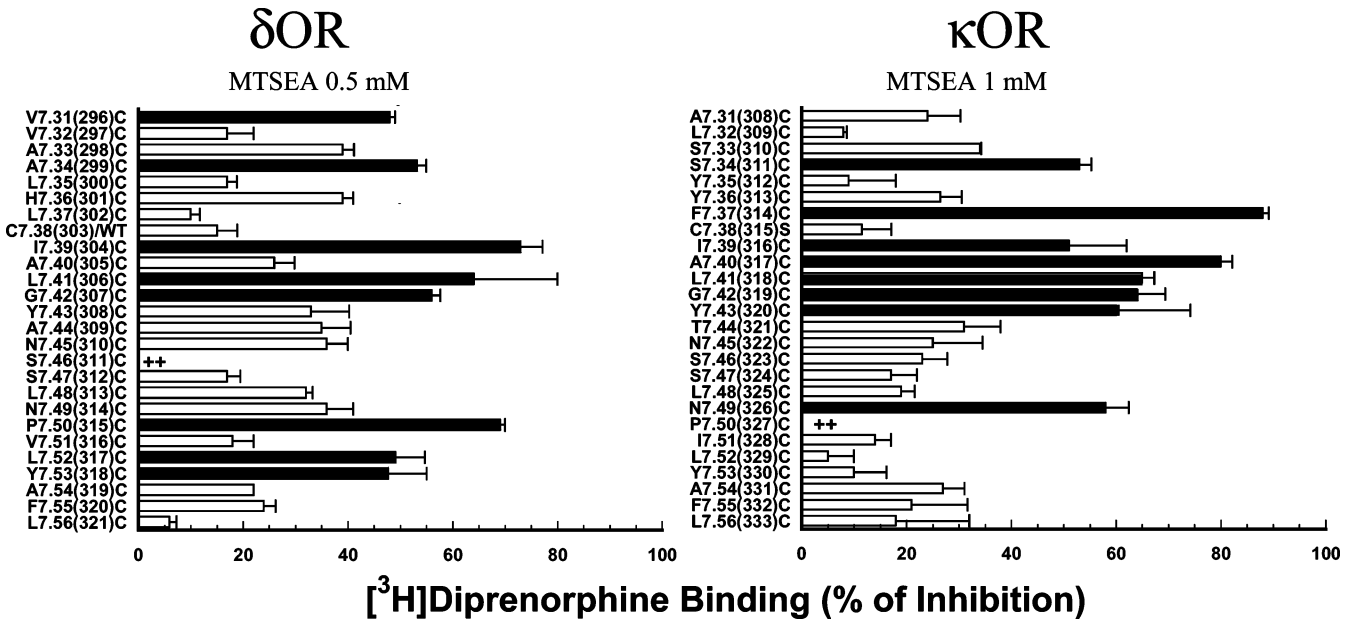

FIGURE 2: SCAM analysis of TM 7 of the δOR and κOR. Inhibition by MTSEA of [^{3}H]diprenorphine binding to the substituted cysteine mutants. Each residue within the TM 7 was mutated to Cys, one at a time, using the wild-type δOR and the κOR C7.38S mutant as the templates. Each of the mutants as well as the templates was expressed in HEK293 cells and treated with indicated concentrations of MTSEA. Cells were washed and assayed for [^{3}H]diprenorphine binding to the receptor in intact cells. Each point represents the mean ± SEM of three to eight experiments in duplicate. Filled bars indicate mutants for which inhibition was significantly different ($p < 0.05$) from the template by one ANOVA followed by post hoc Sheffe *F* test. (++) [^{3}H]Diprenorphine binding was undetectable for S7.46(311)C and P7.50(327)S mutants of the δOR and κOR, respectively.

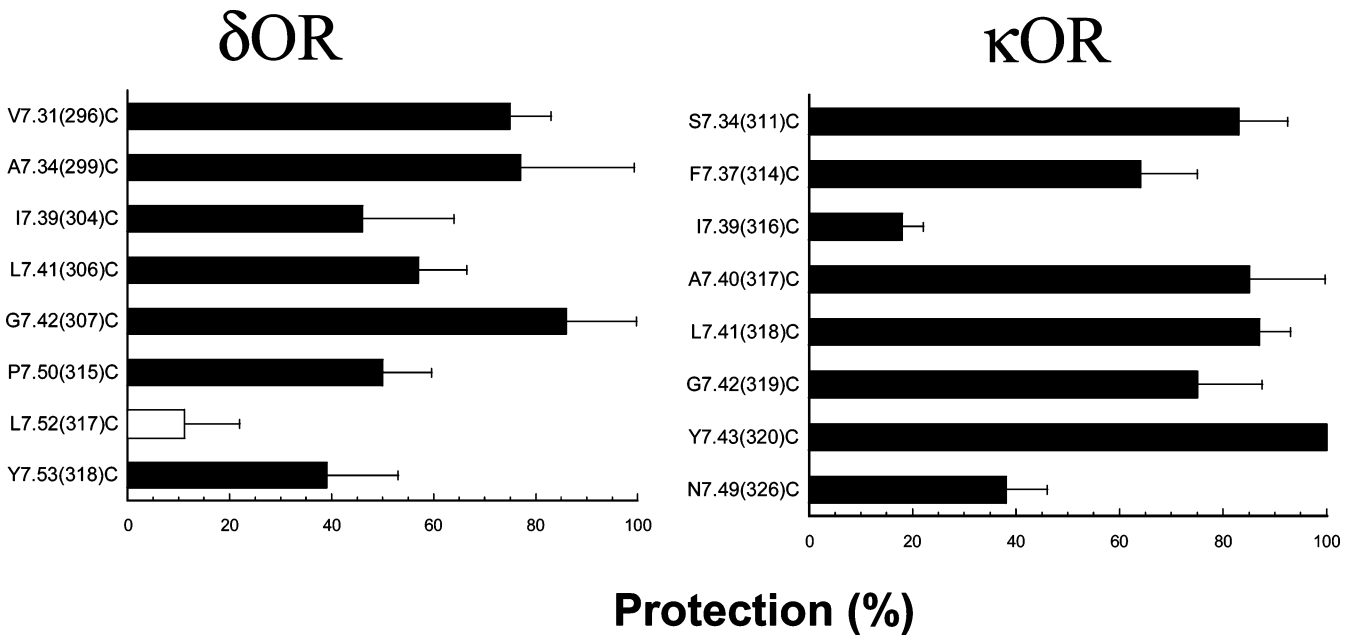

FIGURE 3: Protection by naloxone against inhibitory effects of MTSEA on [^{3}H]diprenorphine binding to MTSEA-sensitive mutants. Each MTSEA-sensitive cysteine-substituted mutant (identified in Figure 2) expressed in HEK293 cells was preincubated with 20 μM naloxone for 20 min at room temperature and then reacted with MTSEA for 5 min at a concentration that caused about 50% of the maximal extent of inhibition for each mutant as determined in Table 3 experiments. Cells were washed and assayed for [^{3}H]diprenorphine binding as described in the Experimental Procedures. Each value represents the mean ± SEM of four to seven experiments in duplicate. Protection was calculated as 1 − (inhibition in the presence of naloxone)/(inhibition in the absence of naloxone). The inhibition in the presence of naloxone was significantly decreased ($p < 0.05$, by paired Student's *t* test) for all of the mutants except L7.52(317)C of the δOR compared with that in the absence of naloxone.

and is not depicted for clarity. Opioid receptors contain the T2.56-X-P2.58 motif in TM2, as the CC chemokine and angiotensin receptors. This motif generates structural differences in the extracellular part of TMs 2 (goldenrod) and 3 (dark red) of the receptor, relative to rhodopsin, without modifying its more compact cytoplasmic surface (*38*, *39*). Thus, TM 2 (goldenrod) is predicted to be in close contact with TM3 (dark red) and not with TM1 (crimson) as in rhodopsin. This also induces the relocation of TM3 (dark red) toward TM5.

Figure 4B shows the amino acid side chains of TM7 (blue) of the δOR and κOR. Green residues represent Cys substitu-

Table 3: Second-Order Rate Constants of the Reaction of $MTSEA^+$ (M^{-1} s^{-1}) with Cysteine-Substituted Mutants of the Human δOR or the Human κOR Transiently Expressed in HEK 293 Cells[a]

	δOR	κOR
7.31C	5.3 ± 0.3	nd[b]
7.34C	6.0 ± 1.2	53.6 ± 6.3
7.37C	nd	62.3 ± 10.2
7.39C	20.16 ± 6.6	472.0 ± 5.1
7.40C	nd	109.1 ± 47.7
7.41C	6.2 ± 3.7	58.6 ± 17.2
7.42C	10.0 ± 0.46	7.3 ± 3.3
7.43C	nd	32.1 ± 5.1
7.44C	nd	nd
7.49C	nd	2.8 ± 0.5
7.50C	10.5 ± 0.6	nd
7.53C	3.6 ± 0.7	nd
background construct	(0.42 ± 0.12)	(<0.4)

[a] Each mutant receptor was incubated with at least four concentrations (in most cases, 0.1, 0.25, 1, and 2.5 mM) of MTSEA for 5 min, and [^{3}H]diprenorphine binding was performed on washed cells. The second-order rate constant (k) for each mutant was calculated as described in the Experimental Procedures. Data represent mean ± SEM of three to six independent experiments in duplicate. [b] nd indicate mutants that are not significantly sensitive to MTSEA as shown in Figure 2.

tions that were sensitive to MTSEA and protected from MTSEA by naloxone pretreatment. Gray residues represent Cys substitutions that MTSEA did not cause any binding inhibition or MTSEA caused binding inhibition but were not protected by naloxone.

DISCUSSION

In this study, we identified by SCAM analysis the residues in the TMs 7 of the δOR and κOR accessible in the binding-site crevices and interpreted the data in the context of rhodopsin-based molecular models of the receptors. To the best of our knowledge, this represents the first study in which such a comparison is made on two closely related receptors. Despite their high sequence homology within the segment examined (17 of 26 residues are identical), the MTSEA sensitivity patterns and reaction rates are very different between the two receptors. The differences are most likely due to the differential interhelical interactions in the δOR and κOR.

κOR and δOR Have Different SCAM Sensitivity Patterns. A cluster of consecutive residues in the middle of TM7 (7.37−7.43) of the κOR are accessible, and many of the residues are not on the same face of the helix (Figure 4B). Among the residues accessible in the binding-site crevice of the δOR, V7.31(296), I7.39(304), G7.42(307), P7.50(315), and Y7.53(318) are on the same face of the helix but A7.34-(299) and L7.41(306) are not (Figure 4B). Because this region is α-helical in the rhodopsin structure, such accessibility patterns are likely due to conformational changes and dynamic movements in this region over the course of the reaction with MTSEA, facilitated by the proline kink at 7.50. In addition, in the κOR, the distance between TM1 and TM7 may be larger (see below), likely rendering residues facing TM1 accessible to MTSEA. MTSEA, the smallest of the MTS reagents, can conceivably penetrate the κOR TM1−TM7 interface, to react with substituted cysteines and interfere with ligand binding. MTSEA has been shown to cross membranes to interact with intracellular cysteines (*46*).

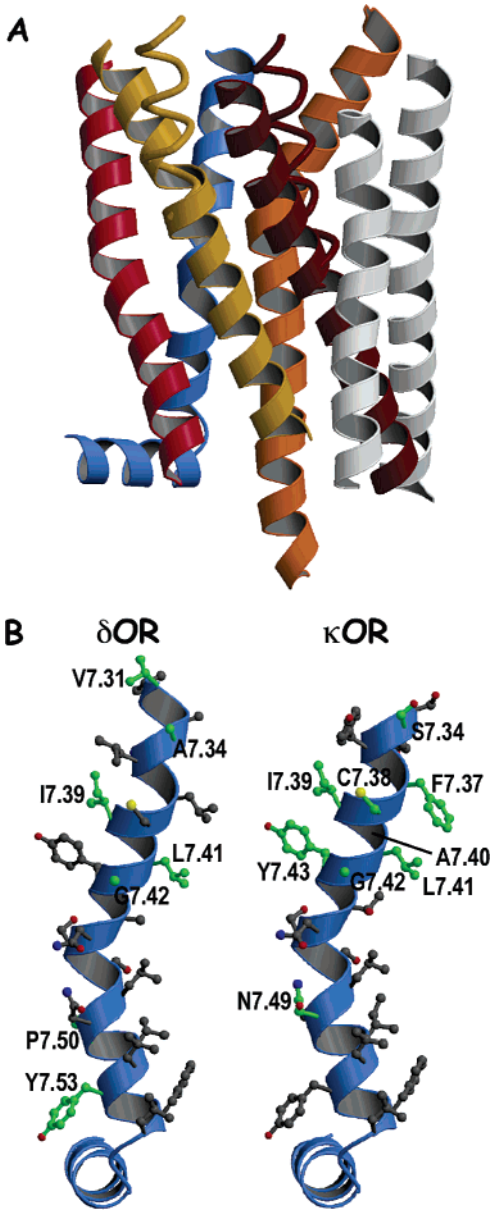

FIGURE 4: Computational models of δOR and κOR. (A) α-Carbon ribbons of transmembrane helices 1 (crimson), 2 (goldenrod), 3 (dark red), 4 (gray), 5 (gray), 6 (orange), and 7 (blue) of rhodopsin (*2*) and transmembrane helices 2 (goldenrod) and 3 (dark red) of the δOR (shown as a tube ribbon). Transmembrane helices 1 and 4−7 are identical in the δOR and rhodopsin. Figures 5−7 use the same color scheme. The κOR is similar to the δOR. (B) Side chains in TMs 7 for the δOR and the κOR depicted in a ball-and-stick representation. Residues ranging from V7.31(296) to L7.56(321) of the δOR and from S7.34(311) to L7.56(333) of the κOR are shown. On the basis of our data, we propose that TM7 starts at 7.31(296) in the δOR but 7.34(311) in the κOR. Green residues depict Cys substitutions that were sensitive to MTSEA and protected from MTSEA by naloxone pretreatment. Gray residues depict Cys substitutions that MTSEA incubation did not inhibit binding or MTSEA caused binding inhibition, but naloxone did not give sufficient protection. P7.50 (green) in the δOR facing away is not visible from this angle. These figures were created using MolScript version 2.1.1 (*66*) and Raster3D version 2.5 (*67*).

For this study, we used intact cells and a 5-min pretreatment period for all experiments to minimize the entry of MTSEA into cells. A 5-min incubation was chosen because the $t_{1/2}$ of MTSEA in aqueous media is about 12 min and 5-min incubation is close to the reaction plateau (*16*).

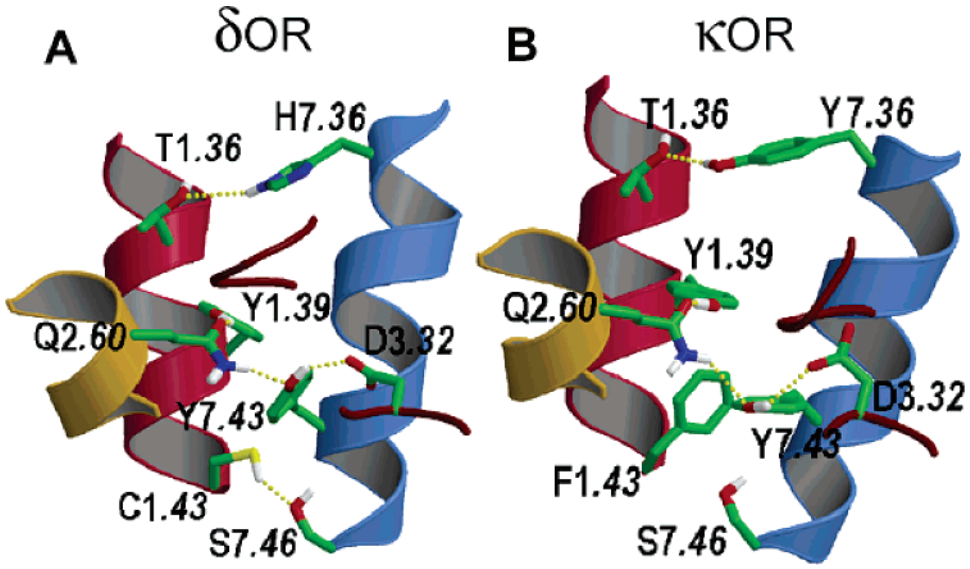

FIGURE 5: Interface between TMs 1 and 7 in the extracellular domain of the δOR (A) and κOR (B). TM1 may be closer to the extracellular half of the TM7 in the δOR than in the κOR because of the presence of the C1.43(60)−S7.46(311) hydrogen bond in the δOR and the need to accommodate the side chain of F1.43(70) between Y1.39(66) and Y7.43(320) in the κOR. This correlates with the shorter side chain of H7.36(301) in the δOR and the longer side chain of Y7.36(313) in the κOR, each forming a hydrogen bond with T1.36. Only polar hydrogens are depicted to offer a better view.

κOR Mutants Have Much Higher Reaction Rates than the δOR Mutants, Except for G7.42C. The overall higher reaction rates of the κOR mutants over the δOR mutants indicate that the previously observed higher rate of C7.38 in the κOR than the δOR (*29*) is part of an overall pattern but not a localized effect. The e2 loops of rhodopsin and the D2 dopamine receptor have been shown to dip into the binding pockets (*1*, *47*). It is possible that the e2 loop of the δ and κ receptors may be similarly positioned in the binding pockets. We (*19*), Wang et al. (*48*), and Meng et al. (*18*) demonstrated previously that the e2 loop of the κOR, containing several Glu and Asp residues, was essential for the high-affinity binding of dynorphin peptides. We have shown that the negative charges in the e2 loop of the κOR may play a role in the higher reaction rates of the κOR by attracting the positively charged MTSEA and accelerating its reaction with the substituted cysteines (*29*). In addition, a longer distance between TM1 and TM7 in the κOR than in the δOR is also an important factor (see below).

Similar Percent of the Wild-Type and Mutant Receptors Is Expressed on the Cell Surface. It has become evident in recent years that a portion of newly synthesized mutant receptors and even wild-type receptors may not be able to exit the endoplasmic reticulum quality-control mechanism to varying extents and are retained in the endoplasmic reticulum (*49*, *50*). One may argue that the observed differential sensitivity may be due to differential surface expression. We thus determined the percent of receptors expressed on the cell surface. A total of 70−80% of each of the wild-type and mutant receptors was found on the cell surface. Therefore, the differential sensitivity to MTSEA observed for the wild-type and mutant receptors is not due to their different subcellular localization. The most likely reason for the similar extents of cell-surface expression is that each construct contains a signal peptide in the N-terminal domain that converts Type IIIa integral membrane protein to Type IIIb, thus enhances insertion of receptors into endoplasmic reticulum, and thus facilitates transport to the Golgi apparatus and plasma membranes (*45*). In studies by Petaja-Repo et al. (*49*, *50*), no such signal peptide was added to the δOR constructs, which may explain the retention of a high percentage of the receptor in the endoplasmic reticulum that they have observed.

Interfaces between TM1 and TM7 Are Different in the δOR and κOR. There are large differences in MTSEA sensitivity and reaction rates in the extracellular portion of the TM7 between the δOR and κOR, indicating significant divergences between the two receptors (parts A and B of Figure 5). The δOR contains C1.43(60) in TM 1, while the κOR has F1.43(70). We found that the δOR S7.46(311)C mutant did not bind [^{3}H]diprenorphine but the S7.46(311)A and the wild-type S7.46(311) did. These results suggest that a disulfide bond may form between C7.46 and C1.43 in the δOR S7.46(311)C mutant, which may distort the binding pocket and thus prevent [^{3}H]diprenphine from binding. In addition, in the wild-type δ receptor, C1.43 and S7.46 may be sufficiently close to form a hydrogen bond, which is much weaker than a disulfide bond, and disruption of this hydrogen bond did not affect binding. In contrast, the F1.43(70) side chain in the κOR is positioned in the face-to-edge orientation (T-shaped) to the aromatic rings of Y1.39(66) and Y7.43(320) (see below), whereas S7.46(323) remains uncoordinated.

The Extracellular Portion of TM1 Is Closer to TM7 in the δOR Than in κOR. The presence of F1.43(70) in the κOR modifies, relative to the δOR, the TM1−7 interface at the extracellular domain of the receptor. The aromatic moiety of F1.43(70) in the κOR interacts in the face-to-edge orientation with both Y1.39(66) and Y7.43(320) (Figure 5B). In contrast, the absence of F1.43(60) in the δOR causes the side chains of Y1.39(56) and Y7.43(308) to form a direct interaction (Figure 5A). This type of $\pi-\sigma$ aromatic−aromatic interaction has been described as an important element of protein structure stabilization (*51*). Figure 8A shows the interatomic distance between the C_α atoms of Y1.39 and Y7.43 in δOR (—) and κOR (- - -) as the computer simulation progresses. Clearly, TM1 in the δOR is located closer to

Table 4: Comparison of TM7 Amino Acids Accessible in the Binding Pockets of the δ and κ Opioid (Current Study), D_2 Dopamine, A_1 Adenosine, and AT_1 Angiotensin II Receptors (*54*−*56*) as Determined by SCAM Analyses

δ opioid receptor	κ opioid receptor	D_2 dopamine receptor	A_1 adenosine receptor	AT_1 angiotensin II receptor
				A7.28(277)
V7.31(296)				V7.31(280)
				T7.33(282)
A7.34(299)	S7.34(311)	L7.34(407)		A7.34(283)
			T7.35(270)	
	F7.37(314)			I7.37(286)
	C7.38(315)	F7.38(411)	A7.38(273)	
I7.39(304)	I7.39(316)	T7.39(412)	I7.39(274)	
	A7.40(317)	W7.40(413)		
L7.41(306)	L7.41(318)			
G7.42(307)	G7.42(319)		T7.42(277)	A7.42(291)
	Y7.43(320)	Y7.43(416)	H7.43(278)	
		N7.45(418)		
	N7.49(326)	N7.49(422)	N7.49(284)	
P7.50(315)		P7.50(423)		
				F7.52(301)
Y7.53(318)		Y7.53(426)	Y7.53(288)	

TM7 (average $C_\alpha-C_\alpha$ distance of 6.9 Å; see gray line in Figure 8A) to establish the direct aromatic interaction between Y1.39(56) and Y7.43(308) than the κOR, in which TM1 is more distant to TM7 (average $C_\alpha-C_\alpha$ distance of 8.2Å) to accommodate the side chain of F1.43(70) between Y1.39(66) and Y7.43(320). In addition, the hydrogen-bond capabilities of the −OH moiety of Y1.39 and Y7.43 in both the δOR and κOR are satisfied by the interactions with the polar side chains of Q2.60 and D3.32. On the basis of their mutagenesis results, Kieffer and colleagues (*23*, *52*) suggest that in the δOR D3.32(128) interacts with Y7.43(308), which is part of the interhelical interactions maintaining the δOR in inactive conformations. The TM1−TM7 distance correlates with the kind of aromatic and polar side chains placed at position 7.36. While the δOR possesses the shorter H7.36(301) side chain to form a hydrogen-bond interaction with the proposed closer T1.36(63) side chain (Figure 5A), whereas the κOR possesses the longer Y7.36(313) side chain to interact with the more distant T1.36(63) (Figure 5B). Consequently, the average $C_\alpha-C_\alpha$ distance between T1.36 and H7.36 in δOR is smaller (9.4 Å, Figure 8B) than the distance obtained between T1.36 and Y7.36 in κOR (10.3 Å, Figure 8B). H7.36C in the δOR and Y7.43C in both the δOR and κOR are poorly expressed (see B_{max} in Tables 1 and 2), indicating the significant role of these side chains in the stability of the TM1−7 interface. Therefore, the patterns of residues in the extracellular portion of TM7 that are accessible to the binding-site crevice are very different in the δOR and κOR (Figure 2 and Tables 3 and 4). The residues of TM7 in the κOR in the interface with TM1 are sensitive to MTSEA (Figure 4C) and possess, in addition, much higher reaction rates than the δ mutants (Table 3) because of the proposed more distant TM1 in this receptor. In contrast, the residues of TM7 in the δOR that are predicted to face TM1 are not sensitive to MTSEA (Figure 4B) probably because of the closer proximity of TM1.

TM7 May Be Longer in δOR Than in κOR. Making the assumption that TM6 extends to position 6.62 (included) and TM7 starts at position 7.33 (included), as observed in the three-dimensional structure of rhodopsin (*2*), the e3 loop is

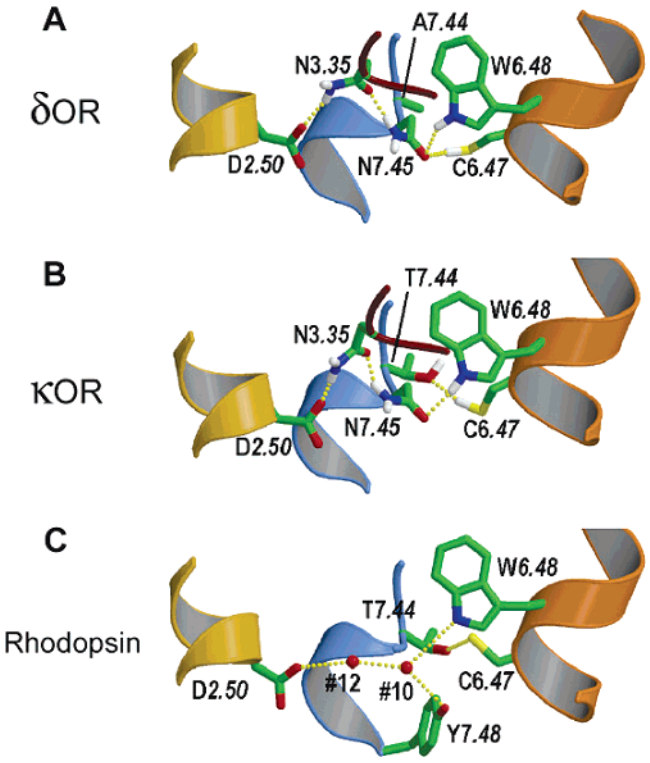

FIGURE 6: Proposed hydrogen-bond network linking D2.50 and W6.48 in the inactive conformation of the δOR (A) and κOR (B) opioid receptors and rhodopsin (C) (*2*). A conserved hydrogen-bond network linking D2.50 and W6.48 includes D2.50, N3.35, N7.45, C6.47, and W6.48 in the δOR and κOR. An additional T7.44(321) is present in the κOR. The crystal structure of rhodopsin has T7.44 and two water molecules (#12 and #10) in place of N3.35 and N7.45.

formed by the I6.63(289)DRRDPLVV7.32(297) sequence in the δOR and by the T6.63(302)SHSTAAL7.32(309) sequence in the κOR. Thus, the putative number of amino acids forming the e3 loop is one residue longer in the δOR than in κOR. In addition, Pro residues are mostly located in loop regions, acting as a helix breaker (*53*). It is, thus, tempting to suggest that TM7 starts at L7.30(295) in the δOR, because of the presence of P7.29(294), and at S7.33(310) in the κOR as in rhodopsin. Therefore, TM7 in the δOR would have an additional helical turn (from 7.30 to 7.33) relative to the κOR and other rhodopsin-like GPCRs (see TM7 in Figure 4B). This is consistent with the finding that MTSEA-sensitive mutants start at position 7.31 in the δOR and at position 7.34 in the κOR (Table 4). In AT1 angiotensin II receptor, MTSEA-sensitive mutants starts at A7.28(277) (*54*), whereas in the D_2 dopamine and A_1 adenosine, receptors starts at L7.34(407) and T7.35(270) (*55*, *56*), respectively. Thus, the TM7 may start at different positions in different GPCRs. The finding that Val7.31(296), Val7.32(297), and Leu7.35(300) are crucial in selectivity of the δOR ligand binding (*57*, *58*) is consistent with these residues being part of the binding pocket.

N7.45 Has a Different Environment in the δOR and κOR: A Conserved Hydrogen-Bond Network Linking D2.50 and W6.48. Figure 6A shows a detailed picture of the N7.45(310) environment of the molecular model of the δOR. The O_δ atom of N7.45(310) acts as a hydrogen-bond acceptor in the interaction with the side chains of both C6.47(273) and W6.48(274). A conformational rearrangement of C6.47 and

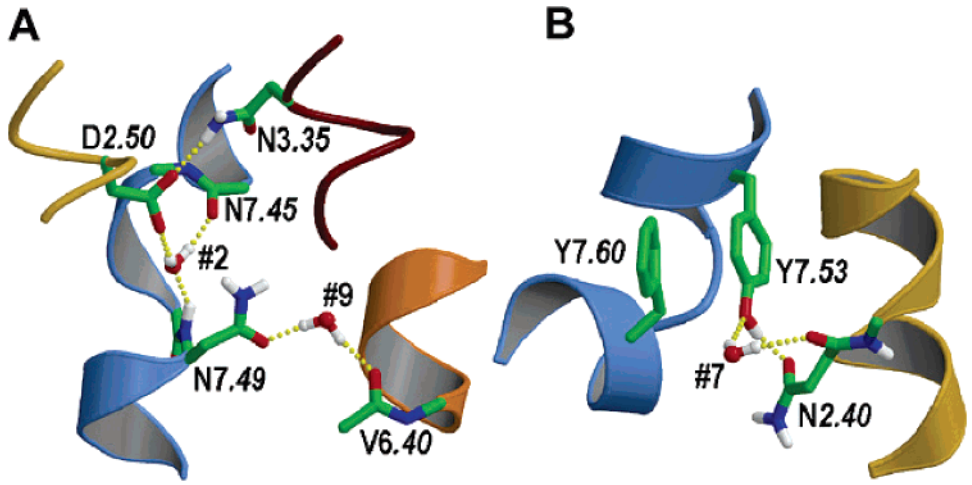

FIGURE 7: Micro-environment of N7.49(314) and Y7.53(318) of the NPXXY motif of the δOR. (A) Detailed view of the proposed hydrogen-bond network at the D2.50/N7.49 environment in the inactive conformation. N7.49 is linked to D2.50 and N7.45 by water #2 and to V6.40 by water #9. (B) Interactions of Y7.53 of the NPxxY motif with the residues located in TM2 and H8. Y7.53(318) interacts with Y7.60(325) in the H8 by an aromatic interaction and links with N2.40(75) by water #7.

W6.48 has been associated with the process of activation of monoamine receptors (*4*, *59*). The conformational change of W6.48 upon receptor activation has been observed in the structure of metarhodopsin I, determined by electron crystallography (*60*). Thus, the role of N7.45 is to restrain C6.47 (χ_1 *trans*) and W6.48 (χ1 *gauche*+) in these rotamer conformations, pointing toward TM7, in the inactive state of the receptor as shown for the histamine H_1 receptor (*61*). Notably, this hydrogen-bond network of interactions is different in the κOR because of the presence of T7.44(321) instead of A7.44(309) in the δOR (Figure 6B). In the κOR, T7.44(321) forms a hydrogen bond with C6.47(286) (as observed in the crystal structure of rhodopsin that lacks N7.45, see below), whereas the O_δ atom of N7.45(322) is dedicated to W6.48(287). While both C6.47 and W6.48 are constrained in the inactive conformation by the single N7.45-(310) amino acid in the δOR, this task is shared by T7.44-(321) and N7.45(322) in the κOR. This different hydrogen-bond network between both types of receptors explains the different levels of B_{max} values observed in the N7.45C mutant receptor (Tables 1 and 2). The N7.45(310)C δOR mutant expressed poorly, whereas the N7.45(322)C κOR mutant expressed well. It is noteworthy that rhodopsin contains C6.47(264), W6.48(265), and T7.44(297) in its sequence but lacks N7.45(298). Rhodopsin fulfills the interactions with C6.47(264) and W6.48(265) through T7.44(297) and water molecule #10 (*2*) (see Figure 6C).

On the other hand, the $N_{\delta 2}-H_2$ moiety of N7.45 interacts with N3.35 in both the δOR and κOR (parts A and B of Figure 6). N3.35 bridges N7.45 and D2.50, acting as a hydrogen-bond donor in the interaction with the side chain of D2.50 and as a hydrogen-bond acceptor in the interaction with N7.45. N3.35 is partly conserved and only present in opioid, bradykinin, formyl-Met-Leu-Phe, somatostatin, angiotensin, C5a anaphylatoxin, and proteinase-activated families of GPCRs. This Asn in the AT1 receptor for angiotensin II plays a critical role in stabilizing the inactive conformation of the receptor (*62*). Importantly, rhodopsin possesses water molecule #12 at the same position as opioid receptors have N3.35, linking D2.50 and water molecule #10 (*2*) (see Figure 6C).

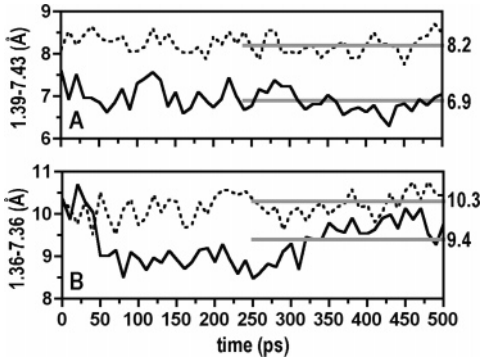

FIGURE 8: Evolution of the interface between TMs 1 and 7 monitored by the interatomic distances between the Cα atoms of (A) Y1.39 and Y7.43 and (B) T1.36 and H/Y7.36 in δOR (—) and κOR (- - -). Gray lines show the average $C_\alpha-C_\alpha$ distance obtained during the production phase of the computer simulations.

Thus, there is a network of interactions between D2.50 and W6.48 (present in 94 and 71%, respectively, of the sequences among family A of GPCRs). However, N3.35 and N7.45 are only conserved in 29 and 67% of the sequences, respectively. Thus, we hypothesize that opioid receptors or other N3.35/N7.45-containing receptors form the D2.50⋯N3.35⋯N7.45⋯W6.48 network of interactions; GPCRs lacking N3.35 form a similar network through D2.50⋯water #12⋯N7.45⋯W6.48 interactions (*61*), and if both N3.35 and N7.45 are absent in the sequence, as in rhodopsin, the D2.50⋯water #12⋯water #10⋯W6.48 (Figure 6C) network links D2.50 and W6.48 (*2*).

Modeling the Environment of the NPxxY Motif in TM7. The environment of the NPxxY motif in the κOR is similar to that in the δOR, and only the δOR is depicted. Figure 7A shows a detailed view of the D2.50(95)/N7.49(314) environment of the molecular model of the δOR. Water molecules #2 and #9 found in the recent structures of rhodopsin are included in the model (*2*, *3*). These structural waters mediate a number of interhelical interactions through the highly conserved D2.50(95) and N7.49(314) amino acids. Water #2 is located between TM2 and TM7, linking the backbone carbonyl of N7.45(310), the backbone N−H amide of N7.49-(314), the side chain of D2.50(95), and the side chain of N7.49(310). Water #9 bridges the side chain of N7.49(310)

and the backbone carbonyl of V6.40(266), keeping the Asn side chain toward TM6. N7.49 plays a central role in the process of receptor activation, acting as an on/off switch by adopting two different conformations in the inactive and active states (*63*, *64*).The role of this active water molecule #9 is to restrain N7.49 in the inactive *gauche*+ conformation, pointing toward TM6 (*3*). We have shown previously that the interaction of D2.50(114) and N7.49(332) in the μ opioid receptor is important for ligand binding and receptor activation (*26*).

Figure 7B shows the interactions of Y7.53(318) with the residues located in TM2 and H8. The aromatic moiety of Y7.53(318) interacts with F7.60(325) in the H8, whereas the hydroxyl group of Y7.53(318) forms hydrogen bonds with the $N_{\delta 2}-H_2$ group and the carbonyl oxygen (via water molecule #7) of the partly conserved N2.40(85) in TM2 (40% of the sequences among family A of GPCRs). The Y7.53C substitution in both the δOR and κOR leads to poorly expressed mutant receptors (Tables 1 and 2). It has been suggested that the Y7.53−F7.60 interaction is disrupted during receptor activation, leading to a proper realigning of H8 (*27*, *28*). In accordance with this model, Decaillot et al. (*52*) demonstrated that the δOR Y7.53(318)H mutant displayed enhanced constitutive activity.

Interpretation of SCAM Results. SCAM analysis has been applied to TMs 7 of D_2 dopamine, AT_1 angiotensin II, and A_1 adenosine receptors (*54*−*56*), in addition to the δOR and κOR in the current study. The residues determined to be accessible in the binding-site crevices in the TMs 7 of these receptors are listed in Table 4.

Although the TMs 7 of the rhodopsin family GPCRs are thought to be helical (*4*, *5*), these receptors have different accessibility patterns and none of them strictly conforms to a pattern consistent with a helical structure. Even between TMs 7 of the δOR and κOR, which are highly homologous with 17 of 26 residues identical, the SCAM sensitivity patterns and MTSEA reaction rates are very different. This is most likely due to different interhelical interactions among these receptors as discussed above. Thus, there is a need to broaden our interpretation of the residues identified in SCAM analysis as being sensitive to MTS reagents. These residues, in addition to those exposed in the binding-site crevices, should also include those accessible from the extracellular medium but not in the binding pocket. Substituted cysteines at latter positions react with MTS reagents, resulting in inhibition of ligand binding indirectly by local steric factors, electrostatic potential, and dynamics of the protein. Therefore, some residues in the TM−TM interface in the outer portion of TMs may be accessible to the extracellular medium. In this region, there are sufficient dynamic movements and/or conformational changes during the course of MTS reagent incubation to allow the reactions to occur. The presence of a ligand such as naloxone probably reduces the dynamic movements and/or conformational changes to decrease reactivity with MTSEA.

Limitations of SCAM. The residues were defined as "sensitive" if the MTSEA reaction at the screening concentration significantly inhibited binding relative to the background, as determined by ANOVA and post hoc testing (see Figure 2). This is a statistical method, and it is imperfect, given that each position will have a different reactivity that is governed by local steric factors, ionization of the cysteine sulfhydryl, electrostatic potential, and dynamics of the protein. In addition, the extent of the inhibition on ligand binding caused by MTSEA modification of a substituted Cys can vary, and therefore, this indirect method of detecting the reaction, although necessary, is also imperfect. Among the sensitive mutants, if naloxone could prevent the reaction with MTSEA, we called the substituted cysteine and, hence the residue mutated, "accessible" in the binding-site crevice.

There are substantial variations in the second-order rate constants among the sensitive cysteine mutants of the δOR or κOR. For example, among the sensitive κ mutants, there is more than a 150-fold difference between the most reactive one [I7.39(316)C, 472.0 ± 5.1 M^{-1} s^{-1} (mean ± SEM, $n = 3$)] and the least reactive one [N7.49(326)C, 2.8 ± 0.5 M^{-1} s^{-1}]. Such a large difference has also been observed in the SCAM analyses of the D2 dopamine receptor (for example, see ref *65*) and results from the factors discussed above. In the case of the least reactive sensitive mutants, only a small margin of reactivity may separate them from mutants deemed insensitive. This is to be expected whenever one uses a statistical definition of accessibility, but this screening method is nonetheless consistent with the rates.

Although using SCAM to probe the receptor structure has its shortcomings, the method has been applied to a number of GPCRs, including the D2 dopamine receptor, A1 adenosine receptor, and AT1 angiotensin II receptors (for example, see refs *5*, *13*, and *54*−*56*), for which no X-ray crystal structures are available. When SCAM analysis is coupled with rhodopsin-based molecular modeling, SCAM analysis has proven to be very useful for elucidating the structures of GPCRs.

ACKNOWLEDGMENT

This work was supported by National Institutes of Health Grants DA 04745, DA11263, and DA17302 to L.-Y.L.-C. and the European Community Sixth Framework Program (LSHB-CT-2003-503337) and CICYT (SAF2004-07103) to L.P.

REFERENCES

1. Palczewski, K., Kumasaka, T., Hori, T., Behnke, C. A., Motoshima, H., Fox, B. A., Le Trong, I., Teller, D. C., Okada, T., Stenkamp, R. E., Yamamoto, M., and Miyano, M. (2000) Crystal structure of rhodopsin: A G protein-coupled receptor, *Science 289*, 739−745.
2. Li, J., Edwards, P. C., Burghammer, M., Villa, C., and Schertler, G. F. (2004) Structure of bovine rhodopsin in a trigonal crystal form, *J. Mol. Biol. 343*, 1409−1438.
3. Okada, T., Fujiyoshi, Y., Silow, M., Navarro, J., Landau, E. M., and Shichida, Y. (2002) Functional role of internal water molecules in rhodopsin revealed by X-ray crystallography, *Proc. Natl. Acad. Sci. U.S.A. 99*, 5982−5987.
4. Visiers, I., Ballesteros, J. A., and Weinstein, H. (2002) Three-dimensional representations of G protein-coupled receptor structures and mechanisms, *Methods Enzymol. 343*, 329−371.
5. Ballesteros, J. A., Shi, L., and Javitch, J. A. (2001) Structural mimicry in G protein-coupled receptors: Implications of the high-resolution structure of rhodopsin for structure−function analysis of rhodopsin-like receptors, *Mol. Pharmacol. 60*, 1−19.
6. Kieffer, B. L. (1995) Recent advances in molecular recognition and signal transduction of active peptides: Receptors for opioid peptides [review], *Cell. Mol. Neurobiol. 15*, 615−635.
7. Knapp, R. J., Malatynska, E., Collins, N., Fang, L., Wang, J. Y., Hruby, V. J., Roeske, W. R., and Yamamura, H. I. (1995) Molecular biology and pharmacology of cloned opioid receptors [review], *FASEB J. 9*, 516−525.

8. Law, P.-Y., Wong, Y. H., and Loh, H. H. (2000) Molecular mechanisms and regulation of opioid receptor signaling, *Annu. Rev. Pharmacol. Toxicol. 40*, 389−430.
9. Strahs, D., and Weinstein, H. (1997) Comparative modeling and molecular dynamics studies of the δ, κ, and μ opioid receptors, *Protein Eng. 10*, 1019−1038.
10. Alkorta, I., and Loew, G. H. (1996) A 3d model of the δ opioid receptor and ligand−receptor complexes, *Protein Eng. 9*, 573−583.
11. Pogozheva, I. D., Lomize, A. L., and Mosberg, H. I. (1998) Opioid receptor three-dimensional structures from distance geometry calculations with hydrogen bonding constraints, *Biophys. J. 75*, 612−634.
12. Metzger, T. G., Paterlini, M. G., Portoghese, P. S., and Ferguson, D. M. (1996) Application of the message-address concept to the docking of naltrexone and selective naltrexone-derived opioid antagonists into opioid receptor models, *Neurochem. Res. 21*, 1287−1294.
13. Javitch, J. A., Shi, L., and Liapakis, G. (2002) Use of the substituted cysteine accessibility method to study the structure and function of G protein-coupled receptors, *Methods Enzymol. 343*, 137−156.
14. Xu, W., Li, J., Chen, C., Huang, P., Weinstein, H., Javitch, J. A., Shi, L., de Riel, J. K., and Liu-Chen, L.-Y. (2001) Comparison of the amino acid residues in the sixth transmembrane domains accessible in the binding-site crevices of μ, δ, and κ opioid receptors, *Biochemistry 40*, 8018−8029.
15. Roberts, D. D., Lewis, S. D., Ballou, D. P., Olson, S. T., and Shafer, J. A. (1986) Reactivity of small thiolate anions and cysteine-25 in papain toward methyl methanethiosulfonate, *Biochemistry 25*, 5595−5601.
16. Karlin, A., and Akabas, M. H. (1998) Substituted-cysteine accessibility method, *Methods Enzymol. 293*, 123−145.
17. Fukuda, K., Kato, S., and Mori, K. (1995) Location of regions of the opioid receptor involved in selective agonist binding, *J. Biol. Chem. 270*, 6702−6709.
18. Meng, F., Hoversten, M. T., Thompson, R. C., Taylor, L., Watson, S. J., and Akil, H. (1995) A chimeric study of the molecular basis of affinity and selectivity of the κ and the δ opioid receptors. Potential role of extracellular domains, *J. Biol. Chem. 270*, 12730−12736.
19. Xue, J. C., Chen, C., Zhu, J., Kunapuli, S., DeRiel, J. K., Yu, L., and Liu-Chen, L.-Y. (1994) Differential binding domains of peptide and non-peptide ligands in the cloned rat κ opioid receptor, *J. Biol. Chem. 269*, 30195−30199.
20. Xue, J. C., Chen, C., Zhu, J., Kunapuli, S. P., de Riel, J. K., Yu, L., and Liu-Chen, L.-Y. (1995) The third extracellular loop of the μ opioid receptor is important for agonist selectivity, *J. Biol. Chem. 270*, 12977−12979.
21. Robinson, P. R., Cohen, G. B., Zhukovsky, E. A., and Oprian, D. D. (1992) Constitutively active mutants of rhodopsin, *Neuron 9*, 719−725.
22. Porter, J. E., Hwa, J., and Perez, D. M. (1996) Activation of the α1b-adrenergic receptor is initiated by disruption of an interhelical salt bridge constraint, *J. Biol. Chem. 271*, 28318−28323.
23. Befort, K., Zilliox, C., Filliol, D., Yue, S., and Kieffer, B. L. (1999) Constitutive activation of the δ opioid receptor by mutations in transmembrane domains III and VII [published erratum appears in *J. Biol. Chem.* Sep 24, 1999, *274* (39), 28058], *J. Biol. Chem. 274*, 18574−18581.
24. Sealfon, S. C., Chi, L., Ebersole, B. J., Rodic, V., Zhang, D., Ballesteros, J. A., and Weinstein, H. (1995) Related contribution of specific helix 2 and 7 residues to conformational activation of the serotonin 5-HT2a receptor, *J. Biol. Chem. 270*, 16683−16688.
25. Zhou, W., Flanagan, C., Ballesteros, J. A., Konvicka, K., Davidson, J. S., Weinstein, H., Millar, R. P., and Sealfon, S. C. (1994) A reciprocal mutation supports helix 2 and helix 7 proximity in the gonadotropin-releasing hormone receptor, *Mol. Pharmacol. 45*, 165−170.
26. Xu, W., Ozdener, F., Li, J.-G., Chen, C., de Riel, J. K., Weinstein, H., and Liu-Chen, L.-Y. (1999) Functional role of the spatial proximity of Asp114(2.50) in TMH 2 and Asn332(7.49) in TMH 7 of the μ opioid receptor, *FEBS Lett. 447*, 318−324.
27. Fritze, O., Filipek, S., Kuksa, V., Palczewski, K., Hofmann, K. P., and Ernst, O. P. (2003) Role of the conserved NPxxY(x)5,6F motif in the rhodopsin ground state and during activation, *Proc. Natl. Acad. Sci. U.S.A. 100*, 2290−2295.
28. Prioleau, C., Visiers, I., Ebersole, B. J., Weinstein, H., and Sealfon, S. C. (2002) Conserved helix 7 tyrosine acts as a multistate conformational switch in the 5HT2C receptor. Identification of a novel "locked-on" phenotype and double revertant mutations, *J. Biol. Chem. 277*, 36577−36584.
29. Xu, W., Chen, C., Huang, P., Li, J., de Riel, J. K., Javitch, J. A., and Liu-Chen, L.-Y. (2000) The conserved cysteine 7.38 residue is differentially accessible in the binding-site crevices of the μ, δ, and κ opioid receptors, *Biochemistry 39*, 13904−13915.
30. Ballesteros, J. A., and Weinstein, H. (1995) Integrated methods for the construction of three-dimensional models and computational probing of structure−function relations in G-protein coupled receptors, *Methods Neurosci. 25*, 366−428.
31. Higuchi, R., Krummel, B., and Saiki, R. K. (1988) A general method of *in vitro* preparation and specific mutagenesis of DNA fragments: Study of protein and DNA interactions, *Nucleic Acids Res. 16*, 7351−7367.
32. Sambrook, J., and Russell, D. W. (2001) *Molecular Cloning: A Laboratory Manual*, Cold Spring Harbor Laboratory Press, Cold Spring Harbor, NY.
33. Li, S., Zhu, J., Chen, C., Chen, Y. W., DeRiel, J. K., Ashby, B., and Liu-Chen, L.-Y. (1993) Molecular cloning and expression of a rat κ opioid receptor, *Biochem. J. 295* (part 3), 629−633.
34. McPherson, G. A. (1983) A practical computer based approach to the analysis of radioligand binding experiments, *Comput. Prog. Biomed. 17*, 107−114.
35. Li, J.-G., Luo, L. Y., Krupnick, J. G., Benovic, J. L., and Liu-Chen, L.-Y. (1999) U50,488H-induced internalization of the human κ opioid receptor involves a β-arrestin- and dynamin-dependent mechanism. κ receptor internalization is not required for mitogen-activated protein kinase activation, *J. Biol. Chem. 274*, 12087−12094.
36. Li, J., Li, J.-G., Chen, C., Zhang, F., and Liu-Chen, L.-Y. (2002) Molecular basis of differences in (−)(trans)-3,4-dichloro-*N*-methyl-*N*-[2-(1-pyrrolidiny)-cyclohexyl]benzeneacetamide-induced desensitization and phosphorylation between human and rat κ-opioid receptors expressed in Chinese hamster ovary cells, *Mol. Pharmacol. 61*, 73−84.
37. Smith, P. K., Krohn, R. I., Hermanson, G. T., Mallia, A. K., Gartner, F. H., Provenzano, M. D., Fujimoto, E. K., Goeke, N. M., Olson, B. J., and Klenk, D. C. (1985) Measurement of protein using bicinchoninic acid, *Anal. Biochem. 150*, 76−85.
38. Govaerts, C., Blanpain, C., Deupi, X., Ballet, S., Ballesteros, J. A., Wodak, S. J., Vassart, G., Pardo, L., and Parmentier, M. (2001) The TXP motif in the second transmembrane helix of CCR5. A structural determinant of chemokine-induced activation, *J. Biol. Chem. 276*, 13217−13225.
39. Govaerts, C., Bondue, A., Springael, J. Y., Olivella, M., Deupi, X., Le Poul, E., Wodak, S. J., Parmentier, M., Pardo, L., and Blanpain, C. (2003) Activation of CCR5 by chemokines involves an aromatic cluster between transmembrane helices 2 and 3, *J. Biol. Chem. 278*, 1892−1903.
40. Canutescu, A. A., Shelenkov, A. A., and Dunbrack, R. L., Jr. (2003) A graph-theory algorithm for rapid protein side-chain prediction, *Protein Sci. 12*, 2001−2014.
41. Kelley, L. A., Gardner, S. P., and Sutcliffe, M. J. (1996) An automated approach for clustering an ensemble of NMR-derived protein structures into conformationally related subfamilies, *Protein Eng. 9*, 1063−1065.
42. Case, D. A., Darden, T. A., Cheatham, T. E., III, Simmerling, C. L., Wang, J., Duke, R. E., Luo, R., Merz, K. M., Wang, B., Pearlman, D. A., Crowley, M., Brozell, S., Tsui, V., Gohlke, H., Mongan, J., Hornka, V., Cui, G., Beroza, P., Schafmeister, C., Caldwell, J. W., Ross, W. S., and Kollman, P. A. (2003) *AMBER8*, University of California, San Francisco, CA.
43. Wang, J. M., Cieplak, P., and Kollman, P. A. (2000) How well does a restrained electrostatic potential (RESP) model perform in calculating conformational energies of organic and biological molecules? *J. Comput. Chem. 21*, 1049−1074.
44. Eisinger, D. A., Ammer, H., and Schulz, R. (2002) Chronic morphine treatment inhibits opioid receptor desensitization and internalization, *J. Neurosci. 22*, 10192−10200.
45. Guan, X. M., Kobilka, T. S., and Kobilka, B. K. (1992) Enhancement of membrane insertion and function in a type IIIb membrane protein following introduction of a cleavable signal peptide, *J. Biol. Chem. 267*, 21995−21998.
46. Holmgren, M., Liu, Y., Xu, Y., and Yellen, G. (1996) On the use of thiol-modifying agents to determine channel topology, *Neuropharmacology 35*, 797−804.

47. Shi, L., and Javitch, J. A. (2004) The second extracellular loop of the dopamine D2 receptor lines the binding-site crevice, *Proc. Natl. Acad. Sci. U.S.A. 101*, 440−445.
48. Wang, J. B., Johnson, P. S., Wu, J. M., Wang, W. F., and Uhl, G. R. (1994) Human κ opiate receptor second extracellular loop elevates dynorphin's affinity for human μ/κ chimeras, *J. Biol. Chem. 269*, 25966−25969.
49. Petaja-Repo, U. E., Hogue, M., Laperriere, A., Walker, P., and Bouvier, M. (2000) Export from the endoplasmic reticulum represents the limiting step in the maturation and cell surface expression of the human δ opioid receptor, *J. Biol. Chem. 275*, 13727−13736.
50. Petaja-Repo, U. E., Hogue, M., Laperriere, A., Bhalla, S., Walker, P., and Bouvier, M. (2001) Newly synthesized human δ opioid receptors retained in the endoplasmic reticulum are retrotranslocated to the cytosol, deglycosylated, ubiquitinated, and degraded by the proteasome, *J. Biol. Chem. 276*, 4416−4423.
51. Burley, S. K., and Petsko, G. A. (1985) Aromatic−aromatic interaction: A mechanism of protein structure stabilization, *Science 229*, 23−28.
52. Decaillot, F. M., Befort, K., Filliol, D., Yue, S., Walker, P., and Kieffer, B. L. (2003) Opioid receptor random mutagenesis reveals a mechanism for G protein-coupled receptor activation, *Nat. Struct. Biol. 10*, 629−636.
53. O'Neil, K. T., and DeGrado, W. F. (1990) A thermodynamic scale for the helix-forming tendencies of the commonly occurring amino acids, *Science 250*, 646−651.
54. Boucard, A. A., Roy, M., Beaulieu, M. E., Lavigne, P., Escher, E., Guillemette, G., and Leduc, R. (2003) Constitutive activation of the angiotensin II type 1 receptor alters the spatial proximity of transmembrane 7 to the ligand-binding pocket, *J. Biol. Chem. 278*, 36628−36636.
55. Fu, D., Ballesteros, J. A., Weinstein, H., Chen, J., and Javitch, J. A. (1996) Residues in the seventh membrane-spanning segment of the dopamine D2 receptor accessible in the binding-site crevice, *Biochemistry 35*, 11278−11285.
56. Dawson, E. S., and Wells, J. N. (2001) Determination of amino acid residues that are accessible from the ligand binding crevice in the seventh transmembrane-spanning region of the human A(1) adenosine receptor, *Mol. Pharmacol. 59*, 1187−1195.
57. Valiquette, M., Vu, H. K., Yue, S. Y., Wahlestedt, C., and Walker, P. (1996) Involvement of Trp-284, Val-296, and Val-297 of the human δ-opioid receptor in binding of δ-selective ligands, *J. Biol. Chem. 271*, 18789−18796.
58. Pepin, M. C., Yue, S. Y., Roberts, E., Wahlestedt, C., and Walker, P. (1997) Novel restoration of function mutagenesis strategy to identify amino acids of the δ-opioid receptor involved in ligand binding, *J. Biol. Chem. 272*, 9260−9267.
59. Shi, L., Liapakis, G., Xu, R., Guarnieri, F., Ballesteros, J. A., and Javitch, J. A. (2002) β2 adrenergic receptor activation. Modulation of the proline kink in transmembrane 6 by a rotamer toggle switch, *J. Biol. Chem. 277*, 40989−40996.
60. Ruprecht, J. J., Mielke, T., Vogel, R., Villa, C., and Schertler, G. F. (2004) Electron crystallography reveals the structure of metarhodopsin I, *EMBO J. 23*, 3609−3620.
61. Jongejan, A., Bruysters, M., Ballesteros, J. A., Haaksma, E., Bakker, R. A., Pardo, L., and Leurs, R. (2005) Linking ligand binding to activation of the histamine H1 receptor, *Nat. Chem. Biol. 1*, 98−103.
62. Auger-Messier, M., Clement, M., Lanctot, P. M., Leclerc, P. C., Leduc, R., Escher, E., and Guillemette, G. (2003) The constitutively active N111G-AT1 receptor for angiotensin II maintains a high affinity conformation despite being uncoupled from its cognate G protein Gq/11α, *Endocrinology 144*, 5277−5284.
63. Govaerts, C., Lefort, A., Costagliola, S., Wodak, S. J., Ballesteros, J. A., van Sande, J., Pardo, L., and Vassart, G. (2001) A conserved Asn in transmembrane helix 7 is an on/off switch in the activation of the thyrotropin receptor, *J. Biol. Chem. 276*, 22991−22999.
64. Urizar, E., Claeysen, S., Deupi, X., Govaerts, C., Costagliola, S., Vassart, G., and Pardo, L. (2005) An activation switch in the rhodopsin family of G protein-coupled receptors: The thyrotropin receptor, *J. Biol. Chem. 280*, 17135−17141.
65. Javitch, J. A., Ballesteros, J., Chen, J., Chiappa, V., and Simpson, M. M. (1999) Electrostatic and aromatic microdomains within the binding-site crevice of the D_2 receptor: Contributions of the second membrane-spanning segment, *Biochemistry 38*, 7961−7968.
66. Kraulis, J. (1991) MOLSCRIPT: A program to produce both detailed and schematic plots of protein structure, *J. Appl. Crystallogr. 24*, 946−950.
67. Merritt, E. A., and Bacon, D. J. (1997) Raster3D: Photorealistic molecular graphics, *Macromol. Crystallogr., B 277*, 505−524.

BI050938A